Published in final edited form as:
J Pediatr Surg. 2012 June ; 47(6): 1143–1149. doi:10.1016/j.jpedsurg.2012.03.020.

Immediate Alterations in Intestinal Oxygen Saturation and Blood Flow Following Massive Small Bowel Resection As Measured By Photoacoustic Microscopy

Kathryn J. Rowland[a,¶], **Junjie Yao**[b,¶], **Lidai Wang**[b,¶], **Christopher R. Erwin**[a], **Konstantin I. Maslov**[b], **Lihong V. Wang**[b,*], and **Brad W. Warner**[a,*]

[a]Division of Pediatric Surgery, St Louis Children's Hospital, Department of Surgery, Washington University School of Medicine, St Louis, MO 63110, USA

[b]Optical Imaging Laboratory, Department of Biomedical Engineering, Washington University in St. Louis, St. Louis, MO 63130, USA

Abstract

Purpose—Massive small bowel resection (SBR) results in villus angiogenesis and a critical adaptation response within the remnant bowel. Previous *ex vivo* studies of intestinal blood flow after SBR are conflicting. We sought to determine the effect of SBR on intestinal hemodynamics using photoacoustic microscopy, a non-invasive, label-free, high-resolution *in vivo* hybrid imaging modality.

Methods—Photoacoustic microscopy was used to image the intestine microvascular system and measure blood flow and oxygen saturation (sO_2) of the terminal mesenteric arteriole and accompanying vein in C57BL6 mice (n=7) prior to and immediately following a 50% proximal small bowel resection. A *p* value of less than 0.05 was considered significant.

Results—Prior to SBR, arterial and venous sO_2 were similar. Immediately following SBR, the venous sO_2 decreased with an increase in the oxygen extraction fraction. In addition, the arterial and venous blood flow significantly decreased.

Conclusion—Massive SBR results in an immediate reduction in intestinal blood flow and increase in tissue oxygen utilization. These physiologic changes are observed throughout the remnant small intestine. The contribution of these early hemodynamic alterations may contribute to the induction of villus angiogenesis and the pathogenesis of normal intestinal adaptation responses.

Keywords

small bowel resection; SBR; oxygen saturation; blood flow; photoacoustic microscopy

*Correspondence: L. V. Wang for photoacoustic imaging, lhwang@biomed.wustl.edu. B. W. Warner for small bowel resection, brad.warner@wustl.edu, St. Louis Children's Hospital, One Children's Place; Suite 5S40, St. Louis MO 63110, (314) 454-6022 – Phone, (314) 454-2442 – Fax.
¶These authors contributed equally to this work

INTRODUCTION

Short gut syndrome is a condition of high morbidity and mortality within the pediatric population and results primarily from massive intestinal loss. After a massive small bowel resection (SBR) in both animal models and humans, a critical adaptation response occurs within the remnant bowel and is characterized by significant increases in villus height and crypt depth, resulting in increased absorptive mucosal surface area to compensate for the attenuated bowel length.

Angiogenesis has long been recognized as important in states of cellular proliferation. The contribution of villus angiogenesis to intestinal adaptation has recently been demonstrated. Proangiogenic growth factor supplementation has been shown to enhance intestinal mucosal growth, and inhibition of vascular endothelial growth factor has resulted in a decreased adaptive response after intestinal loss. Our laboratory has previously established an increased villus capillary density on postoperative day 7 in mice that have undergone massive SBR. This is preceded on postoperative day 3 by an increase in the gene expression of proangiogenic chemokine ligand 5. The exact stimulus for these proangiogenic changes as well as the acute alterations in intestinal hemodynamics following SBR are presently unknown.

Previous *ex vivo* studies of intestinal blood flow at late time points after SBR are conflicting. Studies using intravascular injections of radioactive particles and measurement of radioactivity from harvested tissue as surrogate markers for blood flow have demonstrated increased blood flow following SBR distal to the site of intestinal anastomosis as soon as twenty-four hours following resection, however, the duration of this hyperemic response has been variable. In addition, these studies did not measure other parameters of hemodynamics, including oxygen saturation of hemoglobin (sO_2). No prior studies have measured hemodynamic parameters within the remnant gut immediately after bowel resection using an *in vivo*, real time imaging system with endogenous contrast.

To overcome the limitations of the imaging tools used in prior studies, we sought to determine the effect of SBR on intestinal hemodynamics using photoacoustic microscopy (PAM), a non-invasive, label-free, high-resolution hybrid imaging modality. PAM takes advantage of both rich optical absorption contrast and weak ultrasonic scattering, and thus yields high-contrast images with relatively deep penetration. By spectrally unmixing contributions from various endogenous or exogenous chromophores, PAM is capable of anatomical, functional, and molecular imaging. In particular, because of the excellent signal-to-noise ratio (SNR) provided by hemoglobin, hemodynamic parameters such as vessel density, vessel length, vessel tortuosity, total hemoglobin concentration (C_{Hb}), sO_2, blood flow rate, and metabolic rate of oxygen (MRO_2), have been measured by PAM. With the help of PAM, a better understanding of the acute hemodynamic changes following SBR may further elucidate a mechanism for villus angiogenesis and the pathogenesis of intestinal adaptation.

MATERIALS AND METHODS

Experimental design

A protocol for this study was approved by the Washington University Animal Studies Committee (no 20090275) in accordance with the National Institute of Health laboratory animal care and use guidelines. Mice underwent either 50% proximal SBR (n=7) or sham (enterotomy alone) (n=7) procedure as previously described. Photoacoustic microscopy measurements of the terminal mesenteric arteriole and accompanying vein vessel diameter, blood flow, and oxygen saturation were obtained at 6 cm proximal to the ileal-cecal junction

(ICJ) and at 12 cm proximal to the ICJ on the serosal surface of the intestine both prior to and immediately following the procedure.

Experimental animals

Male mice (C57BL/6; Harlan Laboratories, Inc.; Indianapolis, IN) age 8 to 15 weeks were used in this study. Mice were kept on a 12-hour light-dark cycle and housed in a standard facility. The mice were given free access to standard rodent food pellets and water up until the time of the procedure.

Operative technique

Mice underwent 50% proximal SBR or sham (enterotomy alone) as previously reported with the exception that no reanastamosis was performed. Briefly, a midline laparotomy was made and the bowel was exposed for photoacoustic measurements. Mice that underwent SBR had transection of the bowel at 12 cm proximal to the ICJ and at 1 to 2 cm distal to the ligament of Treitz. The mesentery of the intervening bowel was ligated with a silk tie and the intervening bowel was removed. In mice that underwent the sham procedure, the bowel was transected only at 12 cm proximal to the ICJ.

Intestinal sO_2 and blood flow measured by photoacoustic microscopy

A newly developed fast voice-coil scanning photoacoustic microscopy (VC-PAM) was used throughout this study (Figure 1). Briefly, short laser pulses are focused into the tissue by a set of optical lenses. The resulting photoacoustic signals are detected by an ultrasonic transducer (V2022 BC, Olympus NDT) placed confocally with the optical lens. The whole scanning probe is driven by a voice-coil linear translation stage (VCS-1010, Equipment Solutions, Sunnyvale). The VC-PAM has been demonstrated to be capable of real-time imaging with capillary resolution (transverse: 3.4 μm, axial: 15 μm). An imaging depth of more than 1.2 mm has been achieved in biological tissue. The imaging system is capable of scanning at 20 Hz over a 9 mm range and up to 40 Hz over a 1 mm scanning range.

During the experiment, mice were anesthetized with isoflurane (E–Z Anesthesia, Euthanex) and placed in a supine position on a heating pad (37 °C). A midline laparotomy was performed and the entirety of the small bowel was exposed, The terminal mesenteric artery and accompanying vein at a point approximately 6 cm and 12 cm proximal to the ICJ were identified. Baseline sO_2 was measured at both locations on a 1×4 mm^2 area containing such vessel pairs at two optical wavelengths of 532 nm and 560 nm using a previous publish method. Baseline blood flow speed measurement was then performed at both locations across the proximal end of the vessel in *M*-mode using a bandwidth broadening based method. The laser repetition rate was 10 kHz, and 4000 A-lines were acquired at each position. The area of the bowel not being measured was kept moistened with a normal saline soaked gauze pad. The animal then underwent SBR or sham procedure. Following the procedure, the same artery and vein pairs at 6 cm and 12 cm proximal to the ICJ were imaged with sO_2 and blood flow measurements recorded. Following all measurements the animal was sacrificed via cervical dislocation.

Statistical analysis

All the photoacoustic data processing was conducted using MATLAB (R2008a, MathWorks). Quantitative values are presented as mean ± SEM. An unpaired Student's *t*-test was used for comparisons between all measurements. A p value less than 0.05 was considered to be statistically significant. The Sigma Stat statistical package (SPSS, Chicago, IL) was used for all statistical analyses.

RESULTS

A total of 7 mice underwent the SBR procedure with post-SBR measurements and 7 mice underwent the sham procedure with post-sham measurements. The presented pre-operative data (n=7) represents that of the SBR group only as variability in the pre-operative measurements amongst all animals was minimal. Only data from the measurements recorded at 6 cm proximal to the ICJ is presented as this mid-remnant bowel location best represents the hemodynamic changes throughout the entire remnant small bowel. In all cases the 6 cm measurement agreed with the trend from measurement at the 12 cm proximal to the ICJ location.

Arterial and venous oxygen saturation

Prior to SBR, arterial and venous oxygen saturations (%) were similar (0.98 ± 0.01 arterial pre vs 0.98 ± 0.02 venous pre at 6 cm, *p* value: 0.70). Immediately following SBR, the arterial oxygen saturation decreased (0.98 ± 0.01 pre vs 0.84 ± 0.06 post-SBR at 6 cm, *p* value: <0.05). This trend towards decrease in arterial oxygen saturation was also observed following sham (0.98 ± 0.01 pre vs. 0.95 ± 0.01 post-sham at 6 cm, *p* value: 0.06; Figure 2A).

Venous oxygen saturation dramatically decreased immediately following SBR (0.98 ± 0.02 pre vs 0.66 ± 0.05 post-SBR at 6 cm, *p* value: <0.001). This decrease in venous oxygen saturation was also observed to a lesser degree following sham (0.98 ± 0.02 pre vs 0.86 ± 0.02 post-sham at 6 cm, *p* value: < 0.001). (Figure 2B). The difference between arterial and venous oxygen saturation post-SBR and post-sham was statistically significant, with the venous oxygen saturation decreasing to a greater extent than the arterial (*p* value: <0.05). The pronounced difference in arterial and venous oxygen saturation pre-op and post-SBR are demonstrated in Figure 3.

Tissue oxygen extraction

Tissue oxygen extraction fraction (OEF) is defined as $\left(sO_2^{artery} - sO_2^{vein}\right)/sO_2^{artery}$ and represents the fraction of O_2 molecules that cross the capillary wall. We found that OEF dramatically increased post-SBR (0.01 ± 0.01 pre vs 0.21 ± 0.04 post-SBR at 6 cm, *p* value: < 0.001). OEF also increased post-sham (0.01 +/− 0.01 pre vs 0.09 +/− 0.02 post-sham at 6 cm, *p* value: < 0.05); however, the increase in OEF post-SBR was significantly greater than post-sham (0.21 ± 0.04 post-SBR vs 0.09 ± 0.02 post-sham, *p* value: < 0.05). (Figure 4)

Arterial and venous blood flow

Following SBR, the arterial blood flow decreased (7.6 ± 1.5 mm/s arterial pre vs 2.6 ± 0.55 mm/s post-SBR at 6 cm, *p* value: < 0.05). No change in arterial blood flow was observed in the sham group (7.6 ± 1.5 mm/s arterial pre vs 7.7 ± 0.6 mm/s post-sham, *p* value: 0.93) (Figure 5A).

Venous blood flow also decreased following SBR (4.0 ± 0.7 mm/s venous pre vs 1.6 ± 0.5 mm/s venous post-SBR at 6 cm, *p* value: < 0.05). No change in venous blood flow was observed in the sham group (4.0 ± 0.7 mm/s venous pre vs 4.0 ± 0.5 mm/s venous post-sham, *p* value: 0.98) (Figure 5B).

DISCUSSION

SBR results in villus angiogenesis and intestinal adaptation. While previous studies have attempted to measure changes in blood flow following SBR using *ex vivo* methodologies

and surrogate markers of blood flow, this is the first study to examine the effects of intestinal resection on hemodynamics using an *in vivo* imaging modality (10–12).

The present study demonstrates that PAM is a useful tool for measuring intestinal hemodynamics. The use of hemoglobin as endogenous contrast eliminates the potential disturbance to the intestinal system induced by exogenous contrast. High spatial resolution enables microenvironmental studies down to the level of the capillaries. The spatial resolutions of PAM can also be scaled for deeper tissue imaging. Real-time imaging ability provides for acute response monitoring. In addition, the minimum invasiveness of PAM enables longitudinal studies on the same animal.

The results of the present study demonstrate that at baseline, prior to intervention, arterial and venous sO_2 of the terminal mesenteric artery and accompanying vein are similar. This may indicate minimal to no tissue oxygen utilization of the supplied intestine. Previous *ex vivo* studies of intestinal sO_2 using radioactive microspheres have demonstrated a significant difference between arterial and venous sO_2 in both the fasting and the fed state of other animal models. Stevenson and Weiss record in rats a 93.7% fasted arterial sO_2 in comparison to a 35.8% fasted venous sO_2; fed arterial and venous sO_2 were respectively similar (24). Other studies have demonstrated increased tissue oxygen uptake in piglets following oral feeds (25). In the present study, animals were not fasted prior to measurement, but given free access to standard rodent chow, making the timing of the animal's last meal a variable factor. However, given the minimal variability in the pre-operative measurements of both blood flow and oxygen saturation, this appears to have had minimal effect. While this contradicts previous *ex vivo* studies in other animal models, our *in vivo* results suggest either a high physiologic reserve in mice, and/or left-to-right shunting within the intestinal wall even with a metabolically active state.

Immediately following SBR, hemodynamic changes occur consistent with a reduced oxygen delivery. Venous sO_2 drops dramatically post-SBR. A less dramatic decrease in venous sO_2 also occurs post-sham, likely related to the metabolic effects of transection alone. It is unclear at this point in time the significance of the drop in arterial sO_2 post-SBR and post-sham. However, the overall oxygen extraction fraction post-SBR increases significantly, representing increased tissue oxygen utilization within the remnant bowel. Further, both arterial and venous blood flow decreased post-SBR. Such decrease in blood flow was not seen post-sham and likely represents an immediate reaction to ligation of 50% of the small bowel mesentery and vasculature, and not a reaction to the acute blood loss from the transected marginal artery of the intestine that occurs both post-SBR and post-sham from the associated enterotomy.

Hypoxia is a well-recognized trigger of angiogenesis, resulting in the activation of hypoxia-inducible factors (HIF), responsible for transcriptional activation of genes. In states of intestinal mucosal inflammation, HIFs have been shown to have a protective role. In a study by Karhausen et al, transgenic intestinal epithelial overexpression of HIF-1 protected against trinitrobenzene sulfuric acid-induced colitis, while loss of epithelial HIF-1 resulted in increased colitis severity, weight loss, intestinal permeability, and mortality. It is plausible that cellular changes in response to hypoxia post-SBR may act in a similar manner, having a pro-angiogenic and protective role in the intestinal epithelium.

Previous studies of hemodynamic alterations following SBR have demonstrated a hyperemic response to SBR, however the earliest time point studied in those experiments was 24 hours after resection. In contrast, the data from this study represents changes of the intestinal microvasculature within the first hour post-SBR. It is unclear at this point in time the duration of the hypoxic changes that occur immediately after resection, but further

investigation is underway to determine the changes in hemodynamics that occur as the bowel undergoes adaptation. Our laboratory's previous work has demonstrated an increased villus capillary blood vessel density within the remnant bowel on post-operative day 7. Such new blood vessel growth may be supported by increased blood flow as adaptation occurs.

Intestinal adaptation in response to massive SBR is a multifactorial process involving angiogenesis, cellular proliferation, and apoptosis. Through the use of photoacoustic microscopy, the immediate intestinal hemodynamic changes that occur after SBR, and resultant hypoxia, are novel findings that provide possible mechanistic insight into the changes that occur within the remnant bowel within minutes of resection. The duration of intestinal hypoxia, cellular effects of such hypoxic changes, and impact on villus angiogenesis remain to be studied. A better understanding of hypoxia following SBR and the role of angiogenesis in intestinal adaptation may help in the development of future therapeutic treatments for patients with short gut syndrome.

Acknowledgments

Wang laboratory research was supported by the National Institutes of Health Grants R01 EB000712, R01 EB008085, R01 CA134539, U54 CA136398, R01 EB010049, R01 CA157277, and 5P60 DK02057933. L.V.W. has a financial interest in Microphotoacoustics, Inc. and Endra, Inc., which, however, did not support this work.

Warner laboratory research was support by National Institutes of Health Grants, R01 DK059288 (Warner) and T32 CA009621 (Rowland).

References

1. Helmrath MA, VanderKolk WE, Can G, et al. Intestinal adaptation following massive small bowel resection in the mouse. J Am Coll Surg. 1996; 183:441–449. [PubMed: 8912612]
2. Taylor JA, Martin CA, Nair R, et al. Lessons learned: optimization of a murine small bowel resection model. J Pediatr Surg. 2008; 43:1018–1024. [PubMed: 18558176]
3. McDuffie LA, Bucher BT, Erwin CR, et al. Intestinal adaptation after small bowel resection in human infants. J Pediatr Surg. 2011; 46(6):1045–1051. [PubMed: 21683196]
4. Folkman J. Is angiogenesis an organizing principle in biology and medicine? J Pediatr Surg. 2007; 42:1–11. [PubMed: 17208533]
5. Folkman J. Tumor angiogenesis: therapeutic implications. N Engl JMed. 1971; 285:1182–1186. [PubMed: 4938153]
6. Lee KD, Yamataka A, Kato Y, et al. Basic fibroblast growth factor and granulocyte colony-stimulating factor enhance mucosal surface expansion after adult small bowel transplantation without vascular reconstruction in rats. J Pediatr Surg. 2006; 41:737–741. [PubMed: 16567186]
7. Parvadia JK, Keswani SG, Vaikunth S, et al. Role of VEGF in small bowel adaptation after resection: the adaptive response is angiogenesis dependent. Am J Physiol Gastrointest Liver Physiol. 2007; 293:G591–598. [PubMed: 17585015]
8. Martin CA, Perrone EE, Longshore SW, et al. Intestinal resection induces angiogenesis within adapting intestinal villi. J Pediatr Surg. 2009; 44(6):1077–1082. [PubMed: 19524720]
9. McMellen ME, Wakeman D, Erwin CR, et al. Epidermal growth factor receptor signaling modulates chemokine (CXC) ligand 5 expression and is associated with villus angiogeneis after small bowel resection. Surgery. 2010; 148(2):364–370. [PubMed: 20471049]
10. Ulrich-Baker MG, Hollwarth ME, Kvietys PR, et al. Blood flow responses to small bowel resection. Am J Physiol. 1986; 251(6):G815–822. [PubMed: 3789147]
11. Touloukian RJ, Spencer RP. Ileal blood flow preceding compensatory intestinal hypertrophy. Ann Surg. 1972; 175(3):320–325. [PubMed: 5077796]
12. Jesseph JE, Jacklin AJ. Effects of partial resection of mammalian small intestine. III. Glucose absorption, CO2 production and blood flow in residual ileum in the dog. Rev Surg. 1963; 20:384–387. [PubMed: 14077529]

13. Kim C, Favazza C, Wang LV. In vivo photacoustic tomography of chemicals: high-resolution functional and molecular optical imaging at new depths. Chem Rev. 2010; 110(5):2756–2782. [PubMed: 20210338]
14. Yao J, Maslov K, Hu S, et al. Evans blue dye-enhanced capillary resolution photacoustic microscopy in vivo. J Biomed Opt. 2009; 14(5):054049. [PubMed: 19895150]
15. Maslov K, Zhang HF, Hu S, et al. Optical-resolution photoacoustic microscopy for in vivo imaging of single capillaries. Opt Lett. 2008; 33(9):929–931. [PubMed: 18451942]
16. Wang L, Maslov K, Yao J, et al. Fast voice-coil scanning optical-resolution photoacoustic microscopy. Opt Lett. 2011; 36(2):139–141. [PubMed: 21263479]
17. Wang X, Pang Y, Ku G, et al. Noninvasive laser-induced photoacoustic tomography for structural and functional in vivo imaging of the brain. Nat Biotechnol. 2003; 21(7):803–806. [PubMed: 12808463]
18. Yao J, Maslov KI, Shi Y, et al. In vivo photoacoustic imaging of transverse blood flow by using Doppler broadening of bandwidth. Opt Lett. 2010; 35(9):1419–1421. [PubMed: 20436589]
19. Yao J, Wang LV. Transverse flow imaging based of photoacoustic Doppler badwidth broadening. J Biomed Opt. 2010; 15(2):021304. [PubMed: 20459226]
20. Zhang HF, Maslov K, Sivaramakrishnan M, et al. Imaging of hemoglobin oxygen saturation variations in single vessels in vivo using photoacoustic microscopy. Appl Phys Lett. 2007; 90(5): 053901.
21. Zhang HF, Maslov K, Stoica G, et al. Functional photoacoustic microscopy for high-resolution and noninvasive in vivo imaging. Nat Biotechnol. 2006; 24(7):848–851. [PubMed: 16823374]
22. Yao J, Maslov KI, Zhang Y, et al. Label-free oxygen-metabolic photoacoustic microscopy in vivo. J Biomed Opt. 2011; 16(7):076003–076011. [PubMed: 21806264]
23. Zhang C, Maslov K, Wang LV. Subwavelength-resolution label-free photacoustic microscopy of optical absorption in vivo. Opt Lett. 2010; 35(19):3195–3197. [PubMed: 20890331]
24. Stevenson NR, Weiss HR. Blood flow, O2 extraction and O2 consumption along the rat small intestine. Microvasc Res. 1988; 35(3):278–286. [PubMed: 3134593]
25. Nowicki PT, Stonestreet BS, Hansen NB, et al. Gastrointestinal blood flow and oxygen consumption in awake newborn piglets: effect of feeding. Am J Phsiol. 1983; 245(5 pt 1):G697–702.
26. Cassavaugh J, Lounsbury KM. Hypoxia-mediated biological control. J Cell Biochem. 2011; 112(3):735–744. [PubMed: 21328446]
27. Wang GL, Jiang BH, Rue EA, et al. Hypoxia-inducible factor 1 is a basic-helix-loop-helix-PAS heterodimer regulated by cellular O2 tension. Proc Natl Acad Sci USA. 1995; 92(12):5510–5514. [PubMed: 7539918]
28. Karhausen J, Furuta GT, Tomaszewski JE, et al. Epithelial hypoxia-inducible factor-1 is protective in murine experimental colitis. J Clin Invest. 2004; 114(8):1098–1106. [PubMed: 15489957]

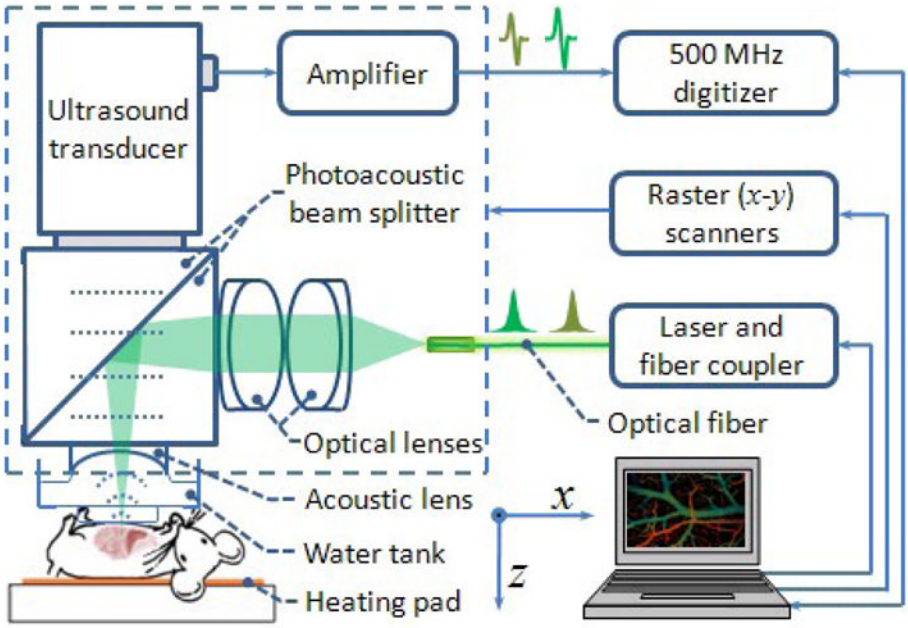

Figure 1.

Schematic of the VC-PAM system and experimental setup. Short laser pulses are focused on the exposed bowel through optical lenses and a homemade photoacoustic beam splitter. Ultrasound signal is collected through an acoustic lens, and the beam splitter. The entire photoacoustic probe (enclosed with dashed square) is attached on to a voice-coil stage and stepper motor stage for raster scanning.

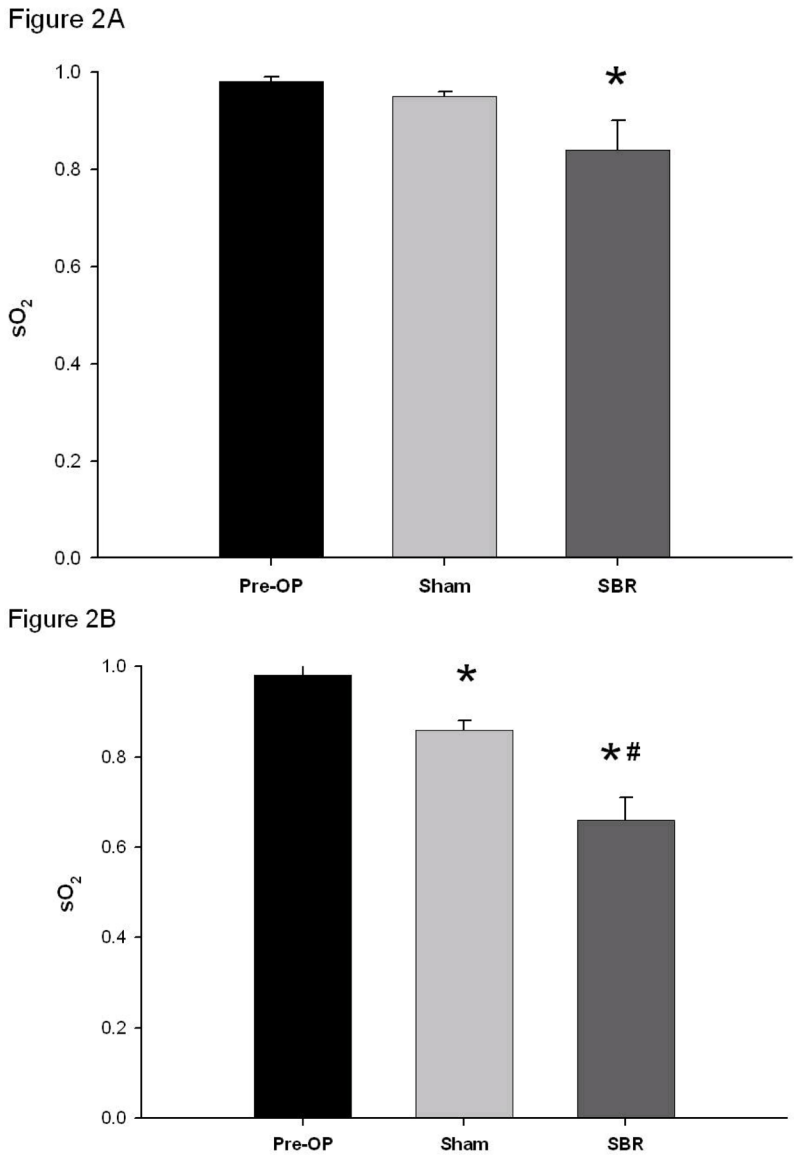

Figure 2.

Oxygen saturation (sO_2) of the terminal mesenteric arteriole (A) and accompanying vein (B) pre-operatively, post-sham (bowel transection alone), and post-SBR at a location 6 cm from the ileal-cecal junction. Asterisk indicates $p < 0.05$ as compared to pre-op (pre-op vs sham and pre-op vs SBR). Number sign indicates $p < 0.05$ sham vs SBR.

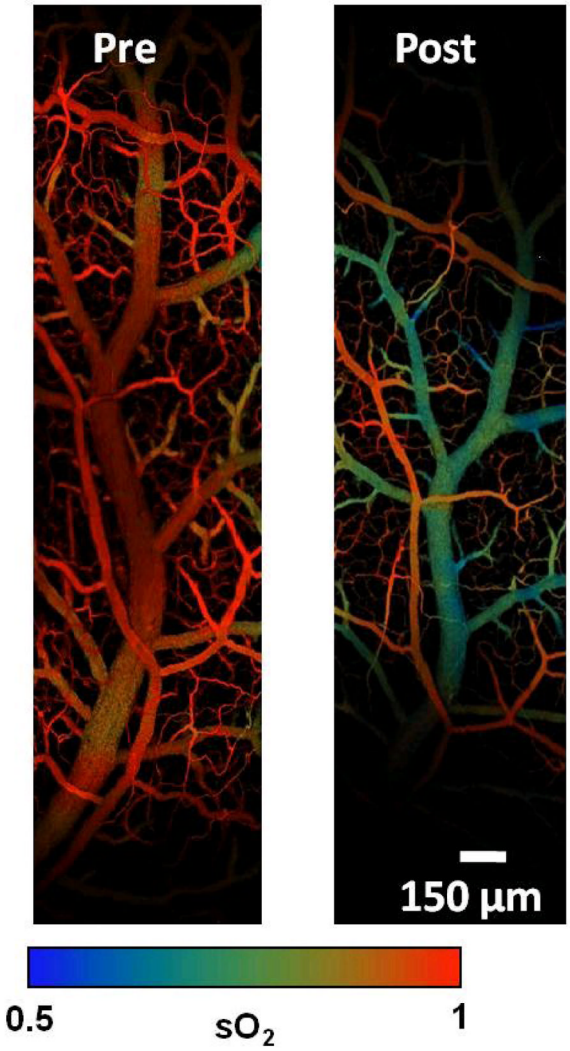

Figure 3.
Photoacoustic microscopy images of intestinal microvascular structure and arterial and venous oxygen saturation (sO_2) pre-operatively and post-SBR.

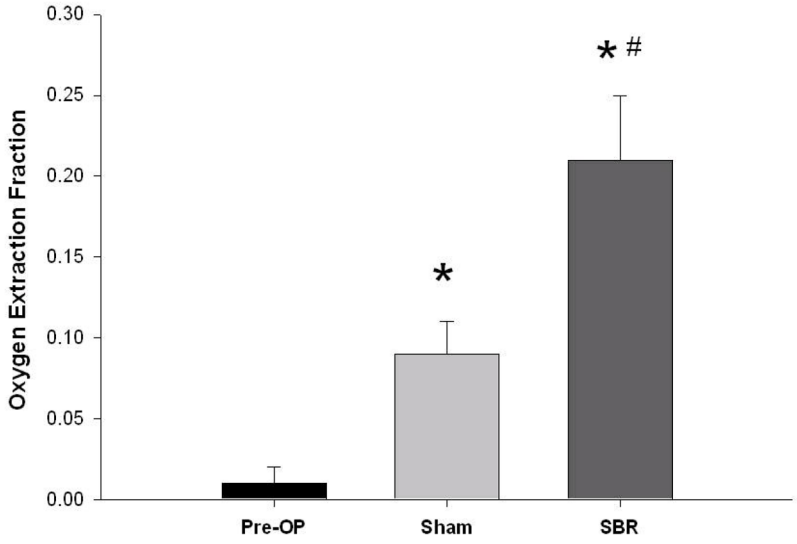

Figure 4.

Tissue oxygen utilization pre-operatively, post-sham, and post-SBR at a location 6 cm from the ileal-cecal junction as calculated by the oxygen extraction fraction. Asterisk indicates $p < 0.05$ as compared to pre-op (pre-op vs sham and pre-op vs SBR). Number sign indicates $p < 0.05$ sham vs SBR.

Figure 5A

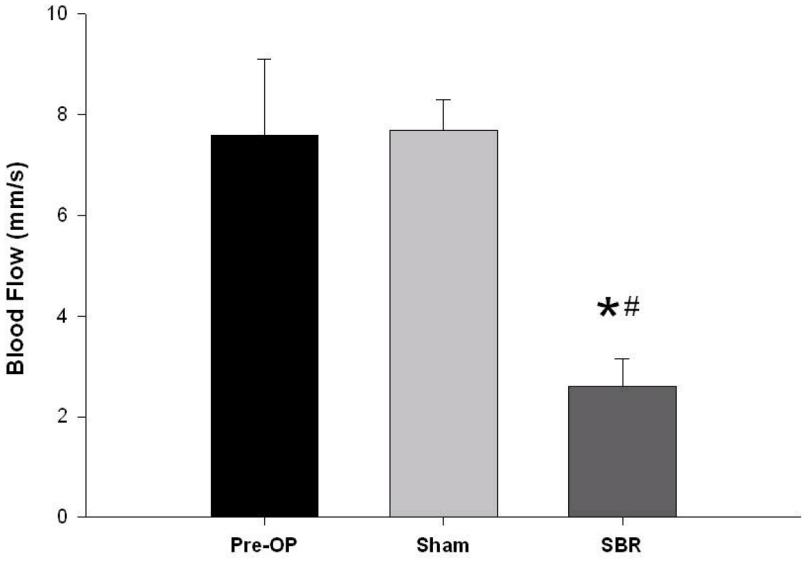

Figure 5B

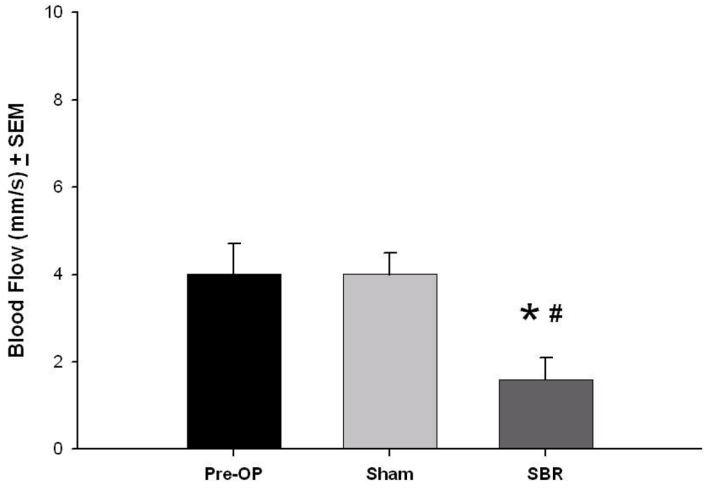

Figure 5.

Blood flow (mm/second) of the terminal mesenteric arteriole (A) and accompanying vein (B) pre-operatively, post-sham, and post-SBR at a location 6 cm from the ileal-cecal junction. Asterisk indicates $p < 0.05$ as compared to pre-op (pre-op vs sham and pre-op vs SBR). Number sign indicates $p < 0.05$ sham vs SBR.